Pergamon

Bioorganic & Medicinal Chemistry 10 (2002) 4143–4154

BIOORGANIC & MEDICINAL CHEMISTRY

Design of Inhibitors of Scytalone Dehydratase: Probing Interactions with an Asparagine Carboxamide

Gregory S. Basarab,[a,*] Douglas B. Jordan,[b] Troy C. Gehret[a] and Rand S. Schwartz[c]

[a]*DuPont Central Research & Development, Experimental Station, Wilmington, DE 19880, USA*
[b]*DuPont Pharmaceuticals Company, Experimental Station, Wilmington, DE 19880, USA*
[c]*DuPont Agricultural Products, Experimental Station, Wilmington, DE 19880, USA*

Received 10 January 2002; accepted 17 May 2002

Abstract—Among the active-site residues of scytalone dehydratase, the side-chain carboxamide of asparagine 131 has the greatest potential for strong electrostatic interactions. Structure-based inhibitor design aimed at enhancing interactions with this residue led to the synthesis of a series of highly potent inhibitors that have a five- or six-membered ring containing a carbonyl functionality for hydrogen bonding. To achieve a good orientation for hydrogen bonding, the inhibitors incorporate a phenyl substituent that displaces a phenylalanine residue away from the five- or six-membered rings. Without the phenyl substituent, inhibitor binding potency is diminished by three orders of magnitude. Larger K_i values of a site-directed mutant (Asn131Ala) of scytalone dehydratase in comparison to those of wild-type enzyme validate the design concept. The most potent inhibitor ($K_i = 15$ pM) contains a tetrahydrothiophenone that can form a single hydrogen bond with the asparagine carboxamide. Inhibitors with a butyrolactam that can form two hydrogen bonds with the asparagine carboxamide demonstrate excellent in vivo fungicidal activity.
© 2002 Elsevier Science Ltd. All rights reserved.

Introduction

Scytalone dehydratase (SD) catalyzes the dehydration of two physiological substrates, scytalone and vermelone, within the fungal melanin biosynthetic pathway employed by certain invasive plant pathogens.[1,2] Catalytic activity of SD is absolutely required for the production of melanin and the initiation of disease by the fungi as genetic and inhibitor knockouts of the enzyme function block melanin production and mitigate fungal penetration into the cells of the host.[3] Hence, SD has been targeted for inhibitor design and optimization programs directed towards discovering crop fungicides. There is considerable information detailing the reactions catalyzed by the enzyme[4–8] and the inhibitors that curtail its activity.[9–15] The several structural classes of inhibitors (e.g., see Fig. 1) that have been reported in the literature accentuate a measure of promiscuity in the SD inhibitor binding pocket, which portends the potential for further structural refinements in the course of inhibitor design.

Three-dimensional structures of SD in complex with each of the inhibitors shown in Fig. 1 have been determined by X-ray crystallography in an iterative fungicide discovery program.[11–13,16,17] The inhibitors are well buried in the enzyme, and the various binding pocket environments have been mapped and visualized as Connolly surfaces. The steric surroundings revealed by the surfaces have led to modifications of the inhibitors to improve binding potency by better occupying the available space.[11] The steric environment has also been used to focus the selection of inputs for a directed combinatorial library of inhibitors, which identified a novel class of low picomolar K_i inhibitors.[13,14] A purposeful displacement of a water molecule associated with the binding pocket by appropriate substitution on another class of inhibitors has been shown to lower K_i's 2- to 20-fold.[5,10] Structures of SD complexed with different inhibitors have revealed conformationally mobile residues within the SD binding pocket leading to the design of new generation inhibitors with modified substituents that displace these residues outward.[12,17]

Improvement in binding potency can be realized by adjusting the fit of the inhibitors in the enzyme through the addition of hydrophobic substituents; as the SD binding pocket is mostly hydrophobic, inhibitor binding

*Corresponding author at present address: AstraZeneca R&D Boston Inc., 35 Gatehouse Drive, Waltham, MA 02451, USA. Tel.: +1-781-839-4689; fax: +1-781-839-4630; e-mail: greg.basarab@astrazeneca.com

0968-0896/02/$ - see front matter © 2002 Elsevier Science Ltd. All rights reserved.
PII: S0968-0896(02)00272-9

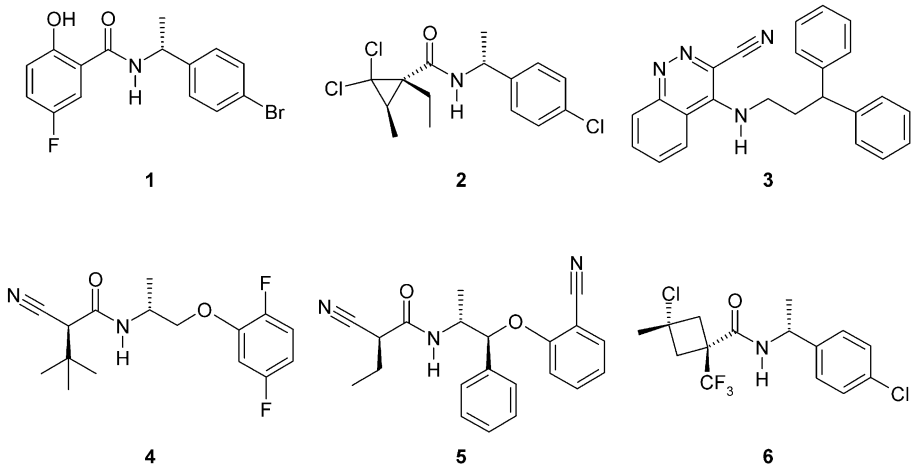

Figure 1. Inhibitors that have been co-crystallized with SD for structure determination by X-ray diffraction.

potency is improved, in part, because the increased hydrophobicity favors partitioning away from the aqueous environment.[18] However, there is a limitation to this means of exploiting the information on the binding pocket in that once the hydrophobicity becomes too high, bioavailability and the expression of fungicidal activity in whole-organism assays is compromised. Hence, it is of practical value to identify more polar inhibitor functionalities that can offer an electrostatic interaction with complementary residues of the SD binding pocket in order to balance the hydrophobic nature of the inhibitors.

Eight SD residues have been demonstrated by kinetic analysis of site-directed mutants to mediate the dehydrations catalyzed by the enzyme.[4,8] Seven of the residues border the inhibitor binding pocket as delineated by the various X-ray structure determinations; the binding constants of a number of inhibitors to the site-directed mutants have been reported as a means of approximating the contributions of the individual residues to the binding potency.[5,15] Overall, Asn131 exhibited the largest influence on inhibitor recognition as determined by the 11- to 1100-fold decrease in binding affinity upon its mutation to alanine.[5,15] Inhibitors such as **1** and **3** display functionalities (the salicylamide hydroxyl and the cinnoline heterocycle, respectively) towards the Asn131 side-chain carboxamide for formation of strong hydrogen bonds, and their binding affinities to SD are profoundly diminished by the mutation to Ala131. In contrast, the binding affinities of inhibitors that display groups (such as the cyclopropyl chlorine atoms of **2** and the nitrile of **4**) of poor hydrogen bonding capability are less affected by the mutation. Neither **1** nor **3** expresses good in vivo disease control in greenhouse assays. There is evidence that **1** is metabolized by both the plant and the fungus for effective detoxification.[19] High lipophilicity of **3** may compromise its bioavailability.

We investigate herein the capability of a more polar carbonyl functionality to share a hydrogen bond with the Asn131 carboxamide in order to boost binding potency. A properly oriented ketone can accept a hydrogen atom from the Asn131 carboxamide as shown in Figure 2A. An inhibitor carboxamide can form two hydrogen bonds with the Asn131 if it is constrained in a ring forcing a *cis* orientation between the carbonyl and NH (Fig. 2B). Inhibitors maintaining these properties are potent inhibitors of SD and constitute effective and novel fungicides.

Results

Molecular modelling

The crystal structures of **4**[11] and **5**[12] in complex with SD were used as the starting points for assembling inhibitor binding models. Replacing the *t*-butyl cyanoacetamide of **4** with a cyclopentanone carboxamide does not allow for the alignment of the ketone functionality for a favorable hydrogen bond with the Asn131 carboxamide without an unfavorable steric clash of the cyclopentanone ring and the side chain of Phe53. This was modeled with a simple MM3 optimization allowing the inhibitor and a 10 Å shell of the surrounding binding pocket to relax.

Compound **5** was designed from the knowledge that there is considerable conformational mobility for Phe53: the phenyl substituent of **5** induced an outward movement of the Phe53 side chain through a π–π stacking arrangement.[12,17] It was reasoned that, with Phe53 displaced away from the cyclopentanone, the impediment towards the alignment of the cyclopentanone carbonyl and the Asn131 carboxamide would be eliminated. Figure 2A depicts the relevant interactions of the cyclopentanone analogue after its replacement for **5** in the crystal structure model, and optimization of a 10 Å shell. The orientation and distances between the cyclopentanone and the Asn131 carboxamide are favorable for alignment of the hydrogen bond: the heteroatom–hydrogen–heteroatom angle that makes up the hydrogen bond is 157° while the heteroatom–heteroatom bond distance is 3.2 Å.

Optimization of a butyrolactam carboxamide replacing compound **5** from its respective crystal structure

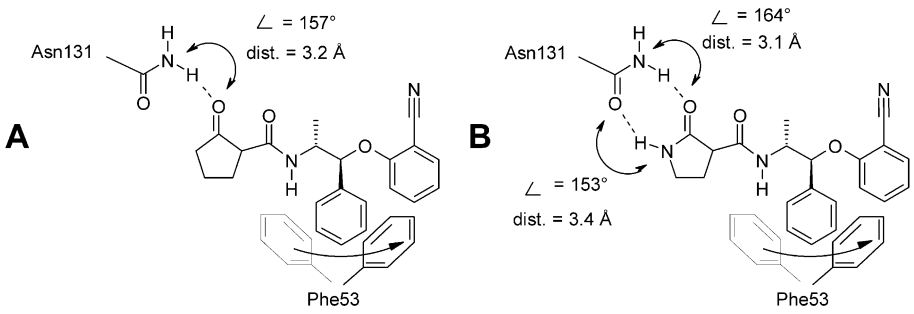

Figure 2. Schematic representation of cyclopentanone (A) and butyrolactam (B) binding interactions with Asn131. Phe53 is displaced away from the cyclopentanone and butyrolactam rings by the inhibitor phenyl substituent.

allowed for formation of two hydrogen bonds. In the model, the Asn131 side chain carboxamide and the lactam carboxamide are nearly co-planar: the root mean square deviation from co-planarity of the eight atoms of the hydrogen bond array of Figure 2B is 0.1 Å. Heteroatom–heteroatom bond distances are acceptable for hydrogen bonding as are the associated hydrogen bond angles.

Synthesis

Amines **8a** and **8b** were derived from norephedrine in a reaction sequence affording a double inversion of stereochemistry to retain the norephedrine configuration (Scheme 1). The norephedrine amine was protected as the phosphonamide. The alcohol was converted to the mesylate, which allowed cyclization to aziridine **7** on treatment with base. The aziridine was opened with the appropriate phenoxide and the protecting phosphonamide was removed with acid treatment. The aziridine ring opening reaction affords some of the alternative regioisomeric products **9a** and **9b**. The protecting phosphonamide group in this sequence serves to activate both aziridine ring formation and aziridine ring opening.

Amine **11** for incorporation into compound **15d** was prepared from the phthalimide protected *d*-alaninol **10** via Mitsunobu reaction with dichlorophenol (Scheme 2).

The syntheses of cyclopentanone, cyclohexanone and tetrahydrothiophenone carboxamides proceeded by protection of the carbonyl of the corresponding keto-esters followed by hydrolysis to the acid and coupling to amines via the acid chlorides (Scheme 3). Deprotection of the carbonyl was achieved with mild acid hydrolysis. The compounds **17**–**19** exist as mixtures of keto and enol tautomers in deuterochloroform with the keto forms existing as 1:1 diastereomeric mixtures.

The butyrolactam carboxylic acid esters **20** and **21** were converted to the desired amides by hydrolysis and EDC coupling with the requisite amines (Scheme 4). The valerolactam carboxylic acid **25** was similarly converted to the amides **26a** and **26b**. Compounds **22a**, **22b**, **26a** and **26b** were each isolated as a 1:1 diastereomeric mixture that was not resolved.

The cyanoacetamide **5b**, an analogue of **5**, was prepared by acylation of **8b** with 2-cyanobutyryl chloride[20] via conditions described previously.[15] The mixtures of **23a** and **24a** and of **23b** and **24b** were separated into the individual diastereomers by chromatography.

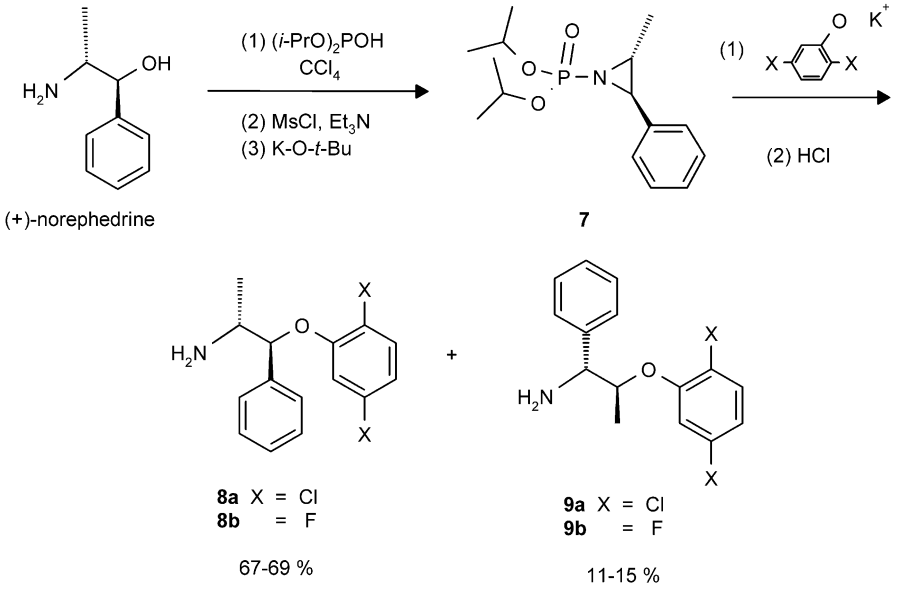

Scheme 1.

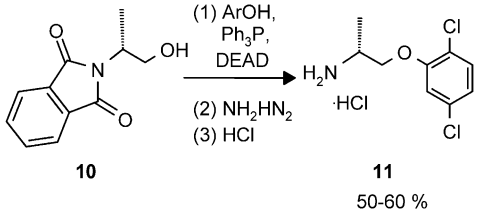

Scheme 2.

Bioefficacy

In order to validate the inhibitor binding model of this work, cyclopentanone carboxamides **17a**, **17c** and **17d** were initially prepared. The chiral bromophenyl amine and phenoxypropyl amine used for the preparations of **17c** and **17d**, respectively, impart high inhibitory potency (K_i's < 50 pM) when coupled to any of the left hand carboxylate derived fragments contained in compounds **1**, **2**, **3**, **4** and **6**.[10–14,17] However, when the amines are incorporated into the cyclopentanone carboxamides **17c** and **17d**, the K_i's are 3–4 orders of magnitude higher (Table 1). Compound **17a** derived from norephedrine has an added phenyl substituent relative to **17d** and shows a 2200-fold improvement in binding potency, in accord with our model.

Cyclopentanone (**17**), cyclohexanone (**18**) and tetrahydrothiophenone (**19**) carboxamides were synthesized to evaluate the relationship of ring size to binding potency (Table 2). From the proton NMR analysis, compounds **17**–**19** exist to varying degrees as a mixture

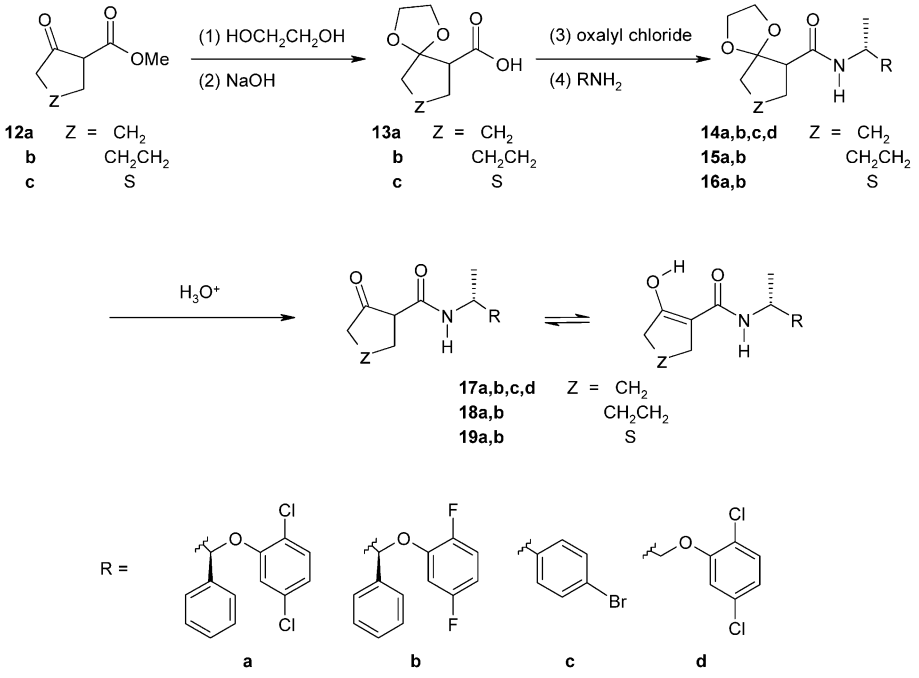

Scheme 3.

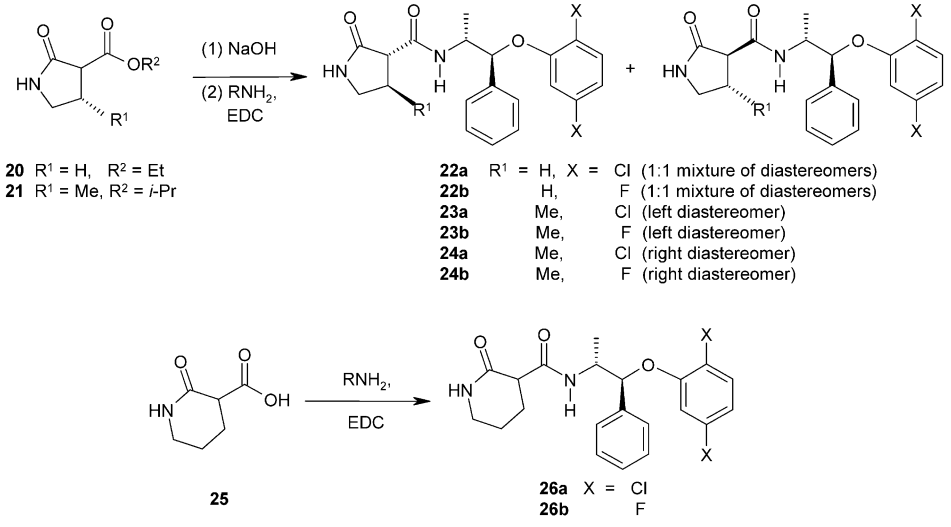

Scheme 4.

Table 1. K_i values of SD and in vivo activity for three cyclopentanone carboxamides

Compound	Structure	K_i (pM)	Sys act @3 ppm	Sys act @0.8 ppm
17a	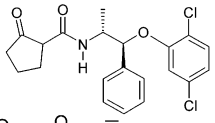	86±8	15	11
17c	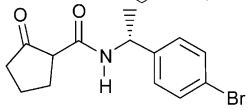	23,000±300	0	0
17d	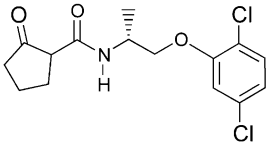	190,000±2000	29	0

of keto and enol tautomers. Each of the keto tautomers further exists as a mixture of diastereomers. It can be presumed that the interconversion of the diastereomers occurs rapidly via the enol tautomer relative to the incubation time (1 min) of the enzyme assay. The tetrahydrothiophenone carboxamides **19**, which are intermediate in ring size to the cyclopentanone and cyclohexanone, showed the highest binding potencies with K_i's ranging from 15 to 16 pM. Both the 2,5-chloro and 2,5-difluoro substitution on the phenoxy group in the analogue series synthesized around **4** and **5** had previously been shown to impart high SD binding potency relative to substitution at other positions or replacement with more polar functionalities.[11,12] Therefore, synthesis of compounds in this work was limited to the 2,5-dihalo substitution.

Table 2. K_i values of SD and in vivo activity for cyclopentanone, cyclohexanone and tetrahydrothiopenone carboxamides

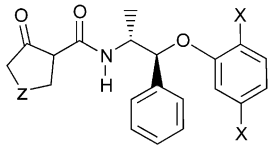

Compound	X	Z	# of diast.	K_i (pM)	Sys. act @3 ppm	Sys. act @0.8 ppm
17a[a]	Cl	CH_2	2	86±8	15	11
17b	F	CH_2	2	71±5	37	0
18a	Cl	CH_2CH_2	2	130±8	0	0
18b	F	CH_2CH_2	2	71±10	13	0
19a	Cl	S	2	16±2	0	0
19b	F	S	2	15±3	27	0

[a]Data repeated from Table 1.

Table 3. K_i values of SD and in vivo activity for butyrolactam and valerolactam carboxamides

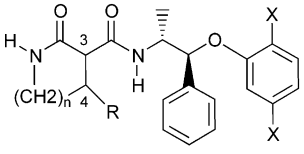

Compound	*n*	*R* (configuration)	X	# of diast.	K_i (pM)	Sys. act @3 ppm	Sys. act @0.8 ppm
22a	1	H	Cl	2	2000±100	0	0
22b	1	H	F	2	460±20	55	42
26a	2	H	Cl	2	3600±100	0	0
26b	2	H	F	2	960±160	17	0
23a	1	CH_3 (4*S*,3*R*)	Cl	1	1000±10	30	33
23b	1	CH_3 (4*S*,3*R*)	F	1	2300±200	44	52
24a	1	CH_3 (4*R*,3*S*)	Cl	1	58±5	97	55
24b	1	CH_3 (4*R*,3*S*)	F	1	110±9	95	92

The cyclic lactam carboxamides **22**, **23**, **24** and **26** (Table 3) exhibited lower binding affinity to SD than compounds **19**, though notably K_i's still ranged from 58 to 3600 pM. The five-member ring lactams **22** and **24** showed higher binding affinity than the six-membered ring compounds **26**. The addition of the methyl group *trans* to the carboxamide improves binding affinity (compare compounds **24a** and **24b** with **22a** and **22b**, respectively). The diastereomers **23** and **24** could be separated by chromatography, and there is no epimerization to the *cis* diastereomers during the course of the enzyme assay. Contamination of the more active isomer in the less active isomer would appreciably overestimate the binding efficacy of the latter though such contamination was not seen within the limits of NMR analysis. The more active diastereomers **24** bind at least 20-fold tighter than the less active. The assignment of the relative stereochemistries of **23a**/**24a** and **23b**/**24b** could not be positively identified though spectroscopic means. The (3*S*,4*R*) configuration about the lactam ring [vs the (4*S*,3*R*) configuration] correlates with the model we have derived and is therefore assigned to the more potent compounds **24a** and **24b**.

A stringent in vivo assay that approximates farm practices was employed to evaluate rice blast disease control.[14] The ratings in Tables 1–3 represent the per cent disease control in a systemic assay in which compound applied to the soil root zone of a rice seedling must translocate to the leaf surface where inoculum is applied. The data from the assay are best interpreted as yes–no results in which disease control above 90% at a given dose represents compound effectiveness while control below 90% is deemed unacceptable for the purpose of disease management (i.e., at the level of commercially viable products). Compounds **24a** and **24b** are the only ones that afford effective control by this assay.

The inhibitor modifications described are targeted at improving the interaction with the side-chain carboxamide of Asn131. Table 4 shows the inhibition constants of compounds **5b**, **19b** and **24b** for the Asn131Ala mutant[4] and wild-type SD to compare the relative importance of displaying a nitrile, a ketone and a carboxamide towards the Asn131 carboxamide. The three compounds of Table 4 are representative of three classes of inhibitors discussed herein. The binding affinity deterioration is greatest (160-fold) for **24b** in going from wild-type SD to the Asn131Ala mutant. In contrast, the affinity of **5b** for the Asn131Ala mutant is only 26-fold less than for wild-type SD.

Discussion

The enzyme binding data support the inhibitor design concept in that improved binding potency was achieved by meshing the interaction of inhibitors with two SD residues (Asn131 and Phe53) that are spatially located in different regions of the binding pocket. Previously, we described the design of **5** (and analogues) starting from compounds such as **4**. In order to accommodate the additional phenyl group of **5**, the *t*-butyl substituent was truncated to an ethyl group as suggested by the binding conformation of the latter delineated by X-ray crystallography.[12] The design involved two modifications of inhibitor structure to achieve higher binding potency. Similarly, there are two important considerations applied to the design of the inhibitors of this work. First, a carbonyl functionality was displayed towards the carboxamide of the side chain of Asn131 to afford a hydrogen bonding capability. The carbonyl was positioned as part of a ring to afford a better steric fit into the binding pocket and to pre-organize the carbonyl into an orientation that allows for a hydrogen bond. In the case of the lactam inhibitors, the ring locks the *cisoid* geometry of the carboxamide NH and carbonyl oxygen necessary for the potential formation of two hydrogen bonds. The second consideration involves the proper choice of the carboxamide *N*-substituent for interaction with Phe53. The SD inhibitory potencies of **17c** and **17d** are lower due to an unfavorable contact

Table 4. K_i values (pM) of wild-type SD and Asn131Ala SD for three carboxamides

Compound	Structure	(A) K_i (Asn131Ala)	(B) K_i (wild-type)	(A)/(B) relative
5b	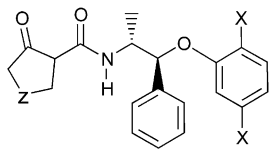	740±10	28±4	26
19b	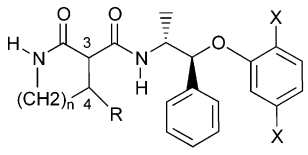	750±180	15±2	50
24b	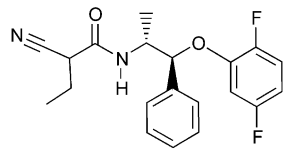	18,000±200	110±9	160

with the side chain of Phe53, which does not allow a favorable alignment of the cyclopentanone carbonyl with Asn131. The phenyl group of Phe53 stacks with the π-face of the unsubstituted phenyl group of the norephedrine derived **17a** and **17b** and enters into a favorable CH–π interaction[21] with the substituted phenoxy group. These interactions relieve the steric congestion around the cyclopentanone five-membered ring and thereby allow for alignment of the hydrogen bond giving rise to the strong binding potency of the inhibitor.

Inhibitor binding involves a number of factors including the contacts to individual protein residues and the energies associated with desolvation of both the inhibitor and the surface of the enzyme binding pocket. The progression of the compounds in Table 4 from **5b** to **19b** to **24b** might be thought to disfavor binding due to the concomitant increase in hydrophilicity, which favors partitioning into the aqueous environment. Though the ketone moiety of **19b** can enter into only one hydrogen bond with the enzyme while the butyrolactam of **24b** can enter into two hydrogen bonds, the binding constant of the latter is higher due to the entropic penalty associated with desolvation of the more polar lactam moiety. Since the enzyme contacts with the five-membered rings of **19b** and **24b** differ from one another and from the ethyl substituted cyanoacetamide fragment of **5b,** evaluation of inhibitor binding constants with the Asn131Ala mutant addresses the role of the Asn131 side-chain carboxamide for recognition of the inhibitors. From this analysis, the better hydrogen bonding of **19b** and **24b** in comparison to **5b** are considered to make up for a loss of hydrophobicity. Though compound **24b** binds less well to SD than **19b** and **5b**, the 160-fold deterioration in binding to Asn131Ala in comparison to wild-type SD indicates that the specific interaction with the side chain carboxamide is strongest among the three compounds. The 50-fold deterioration in binding to Asn131Ala in comparison to wild-type SD indicates that **19b** has a stronger contact with Asn131 than **5b** where the corresponding loss is 26-fold. Hence, the value of comparing inhibitor binding to Asn131Ala and wild-type SD is to dissect apart some of the factors that contribute to the binding phenomenon. Ordinarily, analysis of site-directed mutants serves to delineate catalytic mechanisms of enzyme reactions, as has certainly been exemplified for building a mechanistic hypothesis for SD catalysis.[4,8] Here, inhibitor binding studies on the Asn131Ala mutant serve to substantiate the design thesis: compounds envisioned to provide improved hydrogen bonding capability to the Asn131 carboxamide indeed do so. In the analyses, it is assumed that the desolvation energy associated with the binding of the inhibitors is factored away by the comparison between binding to Asn131Ala and wild-type SD.

Most often in drug design, improvement in binding potency is not the only criterion for superior in vivo performance as bioavailability, metabolism and membrane permeability can degenerate the expression of desired in vivo activity. The interest in finding new classes of chemistry stems from the desire to overcome these hurdles. In going from weak hydrogen bond capability of the nitrile of **5a**, to the improved capability of the carbonyl compounds **17**–**19**, to the further improvement of lactams **22**, **24** and **26**, there is a progression towards increasing hydrophilicity, which has been correlated with improved plant translocation dynamics.[22] Though the ketones **17**–**19** display some of the lower K_i's, they do not exhibit commensurate in vivo activity (see Table 2). They exist as a mixture of keto-enol tautomers, which serve as potential handles for metabolism. That compounds **24a** and**24b** controlled disease in the systemic assay likely reflects their greater hydrophilicity and bioavailability together with the measure of higher binding potency to SD.

In summary, the cyclopentanone, tetrahydrothiophenone and butyrolactams constitute novel pharmacophores for binding to SD leading to novel fungicides. The design of the potent inhibitors goes a step beyond ordinary structure-based design methods by realizing the potential strength of hydrogen bonding to the Asn131 carboxamide from functional studies of the enzyme. Purposely, for obtaining more polar inhibitors with improved in vivo expression of fungicide activity, the more polar substituents of inhibitors were designed to mesh with the Asn131 side chain carboxamide. Proof of the designed interaction with the carboxamide of Asn131 comes from analysis of inhibitor binding constants of the Asn131Ala mutant of SD in comparison to the wild-type SD. This study of SD inhibitors underscores the value of structural studies and site-directed mutagenesis as tools for linking structure to function to practice.

Experimental

Methods and materials

Homogeneous wild-type scytalone dehydratase was purified as described.[23] The homogeneous Asn131Ala mutant of scytalone dehydratase was expressed in *Escherichia coli* and purified as described.[4] All other materials were from Aldrich Chemical (Milwaukee, WI, USA), Sigma Chemical (St. Louis, MO, USA), Hampton (Laguna Hills, CA, USA), Fluka (Buchs, Switzerland), ICN Biomedicals, Inc. (Costa Mesa, CA, USA), or Lancaster Synthesis Inc. (Windham, NH, USA). Chromatographic separations were performed with E. Merck silica gel (230–400 mesh) under nitrogen pressure (flash chromatography). Except where indicated, anhydrous solvents and reagents were used as received. All melting points are uncorrected. ^{1}H NMR spectra where noted, were recorded at 300 MHz. ^{19}F NMR spectra were recorded at 282 MHz. ^{13}C NMR spectra were recorded at 126 MHz. ^{31}P NMR spectra were recorded at 212 MHz. Optical rotation were measured with a Perkin-Elmer model 241 polarimeter. Mass spectra were obtained on a Micromass Platform 2 using Atmospheric Pressure Chemical Ionization detection at 3.5 kV positive ion and 2.5 kV negative ion. Accurate mass elemental composition measurements were performed on a Finnigan MAT900XL mass spectrometer using Electron Multiplier detection at 1.80 kV positive ion and

1.90 kV negative ion. Inhibition constants were determined for both wild-type SD and Asn131Ala via methods described previously with a minimum of three inhibitor concentrations and duplicate activity measurements.[10,15] Protocols for the in vivo assay for determination of disease control have been described.[14]

Synthesis of ((2*R*,3*R*)-3-methyl-2-phenylaziridinyl)bis (methylethoxy)phosphino-1-one (7). A solution of 68 g (215 mmol) of [((2S,1R)-2-hydroxy-1-methyl-2-phenylethyl)amino]bis(methylethoxy)phosphino-1-one[24] and 33 mL (240 mmol) triethylamine in 300 mL ether was cooled in ice water. Methanesulfonyl chloride (18.3 mL, 240 mmol) was added dropwise. The mixture was stirred at room temperature overnight before being diluted with ether and washed with water and brine. Drying ($MgSO_4$) and removal of solvent gave 78 g of an unstable solid, which was used without further purification: mp 121–123 °C; ^{1}H NMR ($CDCl_3$) δ 1.15 (d, 3H), 1.3–1.4 (m, 12H), 2.7 (m, 1H), 2.9 (s, 3H), 3.6–3.7 (m, 1H), 3.8 (s, br, 1H), 4.6 (m, 2H), 5.65 (d, 1H), 7.4 (m, 5H); ^{13}C NMR ($CDCl_3$) δ 16.6, 23.8, 38.8, 52.3, 86.7, 126.6, 127.5, 128.7, 136.2. The solid was dissolved in dry THF cooled in ice water while 30.6 g (280 mmol) of potassium *t*-butoxide was added all at once. After warming to room temperature and stirring for 2 h, the solvent was removed, and the residue was diluted in ether. The ether was washed with water and brine. Drying ($MgSO_4$) and removal of solvent gave 58 g of product as an oil: $[\alpha]_D^{25} = -60.3$ (*c* 1.02, EtOH); ^{1}H NMR ($CDCl_3$) δ 1.2–1.3 (m, 9H), 1.3–1.4 (d, 3H), 1.6 (d, 3H), 2.6 (m, 1H), 3.3–3.4 (dd, 1H), 4.6–4.8 (m, 2H), 7.3 (m, 5H); ^{13}C NMR ($CDCl_3$) δ 15.7, 25.7, 46.1, 46.9, 73.5, 127.8, 129.5, 130.4, 139.6; ^{31}P NMR ($CDCl_3$) δ 9.5; IR (neat) 2979, 2934, 1460, 1419, 1385, 1375, 1263, 1241, 1179, 1142, 1109, 1077, 1063, 1001, 923, 756, 701 cm^{-1}; HRMS calcd for $C_{15}H_{25}NO_3P$ ($M^+ + 1$): 298.1572. Found: 298.1581.

Synthesis of (1*S*,2*R*)-1-(2,5-dichlorophenoxy)-1-phenylprop-2-ylamine hydrochloride (8a). Potassium *t*-butoxide (7.85 g, 70 mmol) was added to a solution of 25.3 g (155 mmol) of 2,5-dichlorophenol in 150 mL DMF at room temperature. Aziridine **7** (23 g, 78 mmol) was added, and the solution was heated at 130 °C for 23 h. The solution was diluted with ether and washed three times with water and once with brine. Drying ($MgSO_4$) and removal of solvent gave a 35 g of a viscous oil. The oil was heated at reflux in 200 mL of 20% aqueous HCl for 2 h. After cooling and diluting with water, the solution was extracted with ether. Insoluble solids were filtered, washed with ether and dried in vacuo to give 12.9 g of product **8a**: mp 209–211 °C; $[\alpha]_D^{25} = -45.7$ (*c* 1.03, EtOH); ^{1}H NMR (DMSO-d_6) δ 1.4 (d, 3H), 3.7 (m, 1H), 5.75 (d, 1H), 6.7 (d, 1H), 6.85 (d, 1H), 7.25 (d, 1H), 7.35 (m, 5H), 8.5 (s, br, 3H); ^{13}C NMR (DMSO-d_6) δ 11.8, 51.3, 79.0, 115.5, 121.5, 122.2, 126.3, 128.6, 128.8, 131.2, 132.0, 135.4, 152.6; IR (KBr) 3452 (br), 3085, 3037, 2999, 2904, 1581, 1497, 1474, 1404, 1255 cm^{-1}; HRMS calcd for $C_{15}H_{16}Cl_2NO$ ($M^+ + 1$): 296.0609. Found: 296.0609. More desired product could be recovered by basifying the aqueous layer with Na_2CO_3 extracting with additional ether. The combined ether layers were dried ($MgSO_4$) and concentrated, and the residue was chromatographed on silica gel. Elution with ether removed a higher R_f component and with ethyl acetate a lower R_f component. Each of the isolated components were dissolved in ether and treated with excess 1N HCl in ether to precipitate solids. The higher R_f component (4.4 g) was identified as (2*S*,1*R*)-2-(2,5-dichlorophenoxy)-1-phenylpropylamine (**9a**) and was characterized as its hydrochloride salt: mp 225–227 °C. $[\alpha]_D^{25} = +36.4$ (*c* 1.02, EtOH); ^{1}H NMR (DMSO-d_6) δ 1.2 (d, 3H), 3.7 (m, 1H), 5.9 (d, 1H), 6.8 (m, 1H), 7.0 (m, 1H), 7.25–7.4 (m, 6H), 8.3–8.4 (s, br, 3H); ^{13}C NMR (DMSO-d_6) δ 15.8, 57.2, 75.5, 116.7, 122.3, 122.4, 128.1, 128.8, 129.3, 131.0, 132.3, 133.4, 152.8; IR (KBr) 3446 (br), 3017, 2983, 2913, 1582, 1502, 1477, 1403, 1260, 1057, 700 cm^{-1}. HRMS calcd for $C_{15}H_{16}Cl_2NO$ [($M^+ - HCl$) + 1]: 296.0609. Found: 296.0622. The lower R_f component corresponded to 2.6 g of additional desired product **8a**.

Synthesis of (1*S*,2*R*)-1-(2,5-difluorophenoxy)-1-phenylprop-2-ylamine hydrochloride (8b). Potassium *t*-butoxide (1.7 g, 15 mmol) was added to a solution of 4.4 g (32 mmol) of 2,5-difluorophenol in 50 mL DMF at room temperature. Aziridine **7** (5.0 g, 17 mmol) was added, and the solution was heated at 130 °C for 21 h. The solution was quenched with aqueous NH_4Cl and extracted with EtOAc. The EtOAc was washed three times with water and once with brine. Drying ($MgSO_4$) and removal of solvent gave a 9 g of a viscous oil. The oil was heated at reflux in 50 mL of 20% aqueous HCl for 2 h. After cooling and diluting with water, the solution was extracted with ether. Insoluble solids were filtered, washed with hexanes and dried in vacuo to give 1.5 g of **8b**, mp 233–235 °C; $[\alpha]_D^{25} = -3.7$ (*c* 1.02, EtOH); ^{1}H NMR (DMSO-d_6) δ 1.2 (d, 3H), 3.7 (m, 1H), 5.9 (d, 1H), 6.8 (m, 1H), 7.0 (m, 1H), 7.25–7.4 (m, 6H), 8.3–8.4 (s, br, 3H); ^{19}F NMR ($CDCl_3$) δ −116, −138; ^{13}C NMR (DMSO-d_6) δ 12.3, 52.6, 80.2, 105.4, 108.6, 117.3, 126.8, 129.0, 129.6, 136.0, 145.7, 149.3 (d, $J = 243$ Hz), 158.2 (d, $J = 241$ Hz); IR (KBr) 3426 (br), 2864, 1511, 1207, 1156, 842, 751, 700 cm^{-1}; HRMS calcd for $C_{15}H_{16}F_2N_2O$ ($M^+ + 1$): 264.1199. Found: 264.1199. More desired product could be recovered by basifying the aqueous layer with Na_2CO_3 extracting additional ether. The combined ether layers were dried ($MgSO_4$) and concentrated, and the residue was chromatographed on silica gel. Elution with ether removed a higher R_f component and with ethyl acetate a lower R_f component. Each of the isolated components were dissolved in ether and treated with excess 1N HCl in ether to precipitate solids. The higher R_f component (0.5 g) was identified as (2*S*,1*R*)-2-(2,5-difluorophenoxy)-1-phenylpropylamine (**9b**) and was characterized as its hydrochloride salt: mp 228–231 °C; $[\alpha]_D^{25} = -10.0$ (*c* 0.94, EtOH) ^{1}H NMR (DMSO-d_6) δ 1.2 (d, 3H), 3.7 (m, 1H), 5.9 (d, 1H), 6.8 (m, 1H), 7.0 (m, 1H), 7.25–7.4 (m, 6H), 8.3–8.4 (s, br, 3H); ^{19}F NMR (DMSO-d_6) δ −116, −137; ^{13}C NMR (DMSO-d_6) δ 15.8, 57.2, 75.6, 105.5, 108.2, 116.7, 128.2, 128.7, 128.9, 133.6, 145.0, 149.4 (d, $J = 240$ Hz), 158.1 (d, $J = 241$ Hz); IR (KBr) 3340 (br), 3040, 3000, 2904, 1625, 1596, 1515, 1459, 1434, 1285, 1206, 1161, 1146, 1101, 1031, 981, 852, 811, 773, 702

cm^{-1}. HRMS calcd for $C_{15}H_{16}F_2NO$ [$(M^+ - HCl) + 1$): 264.1200. Found: 264.1189. The lower R_f component corresponded to 2.6 g of additional desired product **8b**.

Synthesis of 6,9-dioxa-3-thiaspiro[4.4]nonanecarboxylic acid (13c). The carboalkoxyketone **12c**[25] (12 g, 75 mmol), ethylene glycol (4.7 mL, 86 mmol) and 0.5 g *p*-toluenesulfonic acid in 300 mL benzene were heated at reflux overnight with azeotropic removal of water. After dilution with ether, the mixture was washed with water and brine. Drying ($MgSO_4$) and removal of solvent gave an oil that was chromatographed on silica gel (3:1 hexanes–ether) to give 5 g of an oil. The oil was dissolved in 75 mL MeOH along with 2.0 g of 50% NaOH. The solution was heated at reflux overnight. Solvent was removed and the residue was partitioned between aqueous Na_2CO_3 and ether. The ether was separated, and the aqueous phase was extracted again with ether. The aqueous phase was acidified with concd HCl and extracted twice with EtOAc. The EtOAc extracts were washed with brine, dried ($MgSO_4$) and concentrated to give 3.7 g of **13c** as an oil: ^{1}H NMR ($CDCl_3$) δ 2.95–3.1 (m, 4H), 3.2–3.3 (m, 1H), 4.0–4.8 (m, 4H); ^{13}C NMR ($CDCl_3$) δ 25.6, 29.2, 36.6, 38.2, 65.1, 175.4; IR (KBr) 3500 (br), 3056, 2984, 2956, 2897, 2600 (br), 1714, 1421, 1327, 1286, 1229, 1207, 1155, 1126, 1060, 1035, 1005, 950, 911 cm^{-1}; HRMS calcd for $C_7H_{11}O_4S$ ($M^+ + 1$): 191.0378. Found: 191.03852.

General procedure for the synthesis of 17–19

A few drops of DMF were added to a solution of oxalyl chloride (1.2 equiv) and acid **13** (1.1 equiv) in CH_2CH_2. The mixture was heated at reflux overnight. A solution of amine **8** (1.0 equiv) and triethylamine (2.1 equiv) was added, and the resulting mixture was stirred at room temperature overnight. Solvent was removed, and the residue was taken up in EtOAc and washed with water and brine. Drying ($MgSO_4$) and removal of solvent gave an oil, which was dissolved in 1:1 THF–1 N aqueous HCl with stirring overnight. The solution was diluted with EtOAc and washed with water and brine. Drying ($MgSO_4$) and removal of solvent gave an oil, which was chromatographed on silica gel (35% hexanes in ether) to give product.

N-[(2*S*,1*R*)-2-(2,5-Dichlorophenoxy)-1-methyl-2-phenylethyl](2-oxocyclopentyl)carboxamide (17a). Starting with 230 mg of **13a**[26] and 370 mg of **8a**, 380 mg of **17a** was isolated as an oil: $[\alpha]_D^{25} = -5.7$ (*c* 0.98, EtOH); ^{1}H NMR ($CDCl_3$) δ 1.2–1.3 (m, 3H), 1.7–2.4 (m, 6H), 2.9–3.0 (m, 1H), 4.4 (m, 1H), 5.4 (d of d, 1H), 6.6 (2s, 1H), 6.8 (m 1H), 7.0–7.1 (m, 1H), 7.2–7.4 (m, 6H); ^{13}C NMR ($CDCl_3$) δ 13.7 and 13.4, 20.3, 25.9, 38.7, 50.5 and 50.8, 82.7, 115.2 and 115.5, 121.7, 122.3, 126.0, 128.1, 128.7, 130.6, 132.8, 136.8, 154.0, 170.7, 215.8; IR (KBr) 3280, 2980, 2880, 1740, 1630, 1605, 1585, 1480, 1460, 1403, 1266, 1250, 1135, 1100, 1060, 1035, 900 cm^{-1}; HRMS calcd for $C_{21}H_{22}Cl_2NO_3$ ($M^+ + 1$): 406.0977. Found: 406.0992.

***N*-[(2*S*,1*R*)-2-(2,5-Difluorophenoxy)-1-methyl-2-phenylethyl](2-oxocyclopentyl)carboxamide (17b).** Starting with 230 mg of **13a** and 330 mg of **8b,** 240 mg of **17b** was isolated as a solid: mp 82–90 °C; $[\alpha]_D^{25} = +35.9$ (*c* 1.01, EtOH); ^{1}H NMR ($CDCl_3$) δ 1.2–1.3 (m, 3H), 1.8–2.4 (m, 6H), 2.9–3.0 (m, 1H), 4.4 (m, 1H), 5.3 (d of d, 1H), 6.4–6.6 (2m, 1H), 7.0–7.1 (m 2H), 7.2–7.4 (m, 5H); ^{19}F NMR ($CDCl_3$) δ −117, −140; ^{13}C NMR ($CDCl_3$) δ 13.8 and 13.3, 20.4, 25.8, 38.8, 50.7 and 50.5, 54.2, 83.2, 104.8 and 105.0, 107.3 and 107.5, 126.2, 128.2, 128.7, 137.2, 146.8, 149.3 (d, $J = 240$ Hz), 158.4 (d, $J = 239$ Hz), 166.4, 216.0; IR (KBr) 3290, 2990, 2880, 1740, 1630, 1580, 1480, 1455, 1400, 1270, 1250, 1135, 1100, 1060, 1035 cm^{-1}; HRMS calcd for $C_{21}H_{22}F_2NO_3$ ($M^+ + 1$): 374.1568. Found: 374.1557.

***N*-[(1*R*)-1-(4-Bromophenyl)ethyl](2-oxocyclopentyl)carboxamide (17c).** Starting with 200 mg of **13a** and 250 mg of 4-bromo-α-methylbenzylamine hydrochloride, 140 mg of **17c** was isolated as an solid: mp 88–107 °C; $[\alpha]_D^{25} = +109.2$ (*c* 1.03, EtOH); ^{1}H NMR ($CDCl_3$) δ 1.45 (m, 3H), 1.8 (m, 1H), 2.0–2.2 (m, 4H), 2.9 and 3.0 (2t, 1H), 5.0–5.1 (m, 1H), 7.0 (m, br, 1H), 7.1–7.2 (2d, 2H), 7.45 (2d, 2H); ^{13}C NMR ($CDCl_3$) δ; 20.4, 21.9, 22.4, 25.4, 25.7, 35.4, 35.7, 38.9, 47.6, 48.6, 51.8, 54.1, 64.3, 66.0, 71.7, 121.0, 127.9, 131.7, 142.5, 165.8, 216.6; IR (KBr) 3325, 2978, 1738, 1646, 1539, 1491, 1137, 1009, 823 cm^{-1}. HRMS calcd for $C_{14}H_{17}BrNO_2$ ($M^+ + 1$): 310.0443. Found: 310.0433.

***N*-[(1*R*)-2-(2,5-Dichlorophenoxy)-isopropyl](2-oxocyclopentyl)carboxamide (17d).** Starting with 200 mg of **13a** and 270 mg of **11**,[15] 120 mg of **17d** was isolated as a solid: mp 92–98 °C; $[\alpha]_D^{25} = +53.2$ (*c* 0.99, EtOH); ^{1}H NMR ($CDCl_3$) δ 1.35 (m, 3H), 1.7–1.9 (m, 1H), 2.0–2.2 (m, 1H), 2.2–2.5 (m, 4H), 2.95 (q, 1H), 3.9–4.1 (m, 2H), 4.2 (m, 1H), 6.8–7.0 (m, 3H), 7.25 (d, 1H); ^{13}C NMR ($CDCl_3$) δ 17.4, 20.4, 25.9, 38.9, 44.7, 54.2, 71.7, 114.2, 121.7, 130.7, 133.1, 154.7, 154.5, 166.5, 216.2; IR (KBr) 3285, 2979, 2880, 1740, 1646, 1586, 1554, 1484, 1460, 1403, 1266, 1248, 1135, 1096, 1060, 1035, 897, 837 cm^{-1}; HRMS calcd for $C_{15}H_{18}Cl_2NO_3$ ($M^+ + 1$): 330.0664. Found: 330.0649.

N-[(2*S*,1*R*)-2-(2,5-Dichlorophenoxy)-1-methyl-2-phenylethyl](2-oxocyclohexyl)carboxamide (18a). Starting with 250 mg of **13b**[27] and 370 mg of **8a**, 330 mg of **17a** was isolated as a solid: mp 101–114 °C; $[\alpha]_D^{25} = -19.4$ (*c* 1.04, EtOH); ^{1}H NMR ($CDCl_3$) δ 1.2 (m, 3H), 1.6–2.4 (m, 8H), 3.1–3.2 (m, 0.5H), 4.4–4.5 (m, 1H), 5.4 (m, 1H), 5.8 (d, 0.5H),6.6 (m, 1H), 6.85 (t 1H), 7.1–7.4 (m, 6.5H), 14.0 (s, 0.5H); ^{13}C NMR ($CDCl_3$) δ 12.4 and 12.3, 19, 20, 23.1, 26.2, 28, 30.2, 33, 41.1, 49.0, 49.5, 55.0, 63.4, 81.5 and 82.0, 82.5, 19.2, 114.9 and 114.6 and 114.2, 120.8 and 121.0, 124.9, 127.2, 127.8, 129.6, 132.2, 136.0, 163.2, 169.7 and 170.9, 210; IR (KBr) 3403, 2937, 1630, 1605, 1588, 1520, 1484, 1395, 1260, 1220, 1090, 1055, 1000 cm^{-1}; HRMS calcd for $C_{22}H_{24}Cl_2NO_3$ ($M^+ + 1$): 420.1133. Found: 420.1122.

***N*-[(2*S*,1*R*)-2-(2,5-Difluorophenoxy)-1-methyl-2-phenylethyl](2-oxocyclohexyl)carboxamide (18b).** Starting with 250 mg of **13b** and 330 mg of **8b**, 200 mg of **17b** was isolated as a solid: mp 86–92 °C; $[\alpha]_D^{25} = +7.8$ (*c* 1.01, EtOH); ^{1}H NMR ($CDCl_3$) δ 1.2 (m, 3H), 1.7–2.4 (m, 8H), 3.1–3.2 (m, 0.5H), 4.4 (m, 1H), 5.4 (m, 1H), 5.8 (d,

0.5H), 6.6–6.8 (m, 1H), 7.0 (m 1H), 7.2–7.4 (m, 5.5H), 14.0 (s, 0.5H); ^{19}F NMR ($CDCl_3$) δ −117, −140; ^{13}C NMR ($CDCl_3$) δ 13.4, 13.7, 21.9. 22.5, 24.1, 27.2, 28, 29.3, 31.3, 33, 36, 42.0, 49.8, 50.3, 50.5, 55.9, 83.1, 83.3, 83.8, 96.9, 104, 107, 116, 126.0, 126.2, 128.2, 128.7, 137.2, 146.8, 150 (d, J = 240 Hz), 159 (d, J = 240 Hz), 168.6, 170.8, 171.9, 210.0; IR (KBr) 3395, 2940, 1630, 1605, 1583, 1520, 1478, 1396, 1261, 1223, 1094, 1056, 999 cm^{-1}; HRMS calcd for $C_{22}H_{24}F_2NO_3$ ($M^+ + 1$): 388.1724. Found: 388.1713.

***N*-[(2*S*,1*R*)-2-(2,5-Dichlorophenoxy)-1-methyl-2-phenylethyl](4-oxo(3–2,3,5-trihydrothienyl))carboxamide (19a).** Starting with 260 mg of **13c** and 370 mg of **8a**, 110 mg of **19a** was isolated as a solid: mp 90–98 °C; $[\alpha]_D^{25} = -41.4$ (c 1.02, EtOH); ^{1}H NMR ($CDCl_3$) δ 1.2–1.3 (m, 3H), 3.2–3.8 (m, 4.75H), 4.35–4.55 (m, 1H), 5.3–5.4 (dd, 1H), 5.6 (d, 0.25H), 6.6 (m, 1H), 6.8–6.9 (m 1H), 7.0–7.1 (m, 0.75H), 7.2–7.4 (m, 6H), 12.8 (s, 0.25H); ^{13}C NMR ($CDCl_3$) δ 13.1 and 13.3, 27, 30.7, 35.9, 42.4, 49.7 and 49.9 and 50.7; 54.8 and 56.4, 82.4 and 83.6, 100.1, 115.2 and 115.4 and 115.8, 121.6 and 121.7 and 122.1, 125.6 and 125.8, 128.1 and 128.2, 128.6 and 128.8, 130.5, 136.5, 165; IR (KBr) 3410, 2940, 1720 1630, 1605, 1587, 1505, 1480, 1395, 1260, 1220, 1090, 1055, 1000 cm^{-1}; HRMS calcd for $C_{20}H_{20}Cl_2NO_3S$ ($M^+ + 1$): 424.0541. Found: 424.0527.

***N*-[(2*S*,1*R*)-2-(2,5-Difluorophenoxy)-1-methyl-2-phenylethyl](4-oxo(3–2,3,5-trihydrothienyl))carboxamide (19b).** Starting with 260 mg of **13c** and 330 mg of **8b**, 100 mg of **19b** was isolated as an oil: $[\alpha]_D^{25} = -17.5$ (c 1.04, EtOH); ^{1}H NMR ($CDCl_3$) δ 1.2–1.3 (m, 3H), 3.2–3.8 (m, 4.75H), 4.4 (m, 1H), 5.3 (m, 1H), 5.6 (d, 1H), 6.4–6.6 (m, 2H), 7.1–7.2 (m 1.75H), 12.8 (s, 0.25H); ^{19}F NMR ($CDCl_3$) δ −117, −140; ^{13}C NMR ($CDCl_3$) δ 13.4, 13.5, 16.5, 28.6, 30.8, 36.1, 38.8, 42.3, 49.7, 50.1, 50.6, 50.9, 55.0, 83.2, 84.1, 98, 100.3, 104.4, 104.6, 107.1, 107.3, 116.3, 126.1, 128.3, 128.8, 136.9, 159.3, 157.4, 156.4, 146, 148, 150, 164.7, 171.4, 109.2; 3390, 2941, 1720 1630, 1605, 1590, 1520, 1484, 1395, 1260, 1220, 1090, 1050, 1000 cm^{-1}; HRMS calcd for $C_{20}H_{19}F_2NO_3S$ ($M^+ + 1$): 392.1131. Found: 392.1126.

Synthesis of *N*-[(2*S*,1*R*)-2-(2,5-dichlorophenoxy)-1-methyl-2-phenylethyl](2-oxopyrrolidin-3-yl)carboxamide (22a). A solution of 180 mg (1.4 mmol) pyrrolidinone carboxylate **20**,[28] 0.39 mL (2.8 mmol) triethylamine, 465 mg (1.4 mmol) **8a**, and 270 mg (1.4 mmol) ethyl-3(3-dimethylamino)propyl carbodiimide (EDC) in 10 mL CH_2CH_2 was stirred at room temperature overnight. The solution was washed with water and brine, dried ($MgSO_4$) and concentrated. The residue was chromatographed on silica gel (EtOAc) to give product as a 1:1 mixture of diastereomers as an oil: $[\alpha]_D^{25} = -13.8$ (c 0.99, EtOH); ^{1}H NMR ($CDCl_3$) δ 1.2–1.3 (2d, 3H), 2.3–2.7 (m, 2H), 3.2 (m, 1H), 3.4 (m, 2H), 4.4 (m, 1H), 5.4 (dd, 1H), 5.6–5.7 (d, br 1H), 6.6 (s, 1H), 6.8 (m, 1H), 7.2–7.4 (m, 6H), 7.7–7.9 (2d, 1H); ^{13}C NMR ($CDCl_3$) δ 13.4, 13.5, 28.7, 36, 38.8, 50.1, 50.8, 51.0, 55, 82.7, 83.8, 115.3, 115.6, 121.8, 122.0, 125.8, 126.0, 128.3, 128.8, 129.0, 130.7, 154.0, 164.8, 167.2, 171.5, 209.1; IR (CH_2CH_2) 3420 (br), 3280 (br), 1700, 1662, 1580, 1540, 1480, 1450, 140, 1375, 1261, 1094, 1060, 995 cm^{-1}; HRMS calcd for $C_{20}H_{21}$ $Cl_2N_2O_3$ ($M^+ + 1$): 407.0929. Found: 407.0941.

Synthesis of *N*-[(2*S*,1*R*)-2-(2,5-difluorophenoxy)-1-methyl-2-phenylethyl](2-oxopyrrolidin-3-yl)carboxamide (22b). A solution of 180 mg (1.4 mmol) pyrrolidinone carboxylate **20**, 0.39 mL (2.8 mmol) triethylamine, 420 mg (1.4 mmol) **8b**, and 270 mg (1.4 mmol) EDC in 10 mL CH_2CH_2 was stirred at room temperature overnight. The solution was washed with water and brine, dried ($MgSO_4$) and concentrated. The residue was chromatographed on silica gel (EtOAc) to give product as a 1:1 mixture of diastereomers as an oil: $[\alpha]_D^{25} = +29.7$ (c 1.14, EtOH); ^{1}H NMR ($CDCl_3$) δ 1.2–1.3 (2d, 3H), 2.3–2.7 (m, 2H), 3.2 (m, 1H), 3.4 (m, 2H), 4.4 (m, 1H), 5.3 (dd, 1H), 5.7 (d, br 1H), 6.5 (m, 2H), 7.0 (m, 1H), 7.2–7.4 (m, 5H), 7.8 (2d, 1H); ^{19}F NMR ($CDCl_3$) δ −117, −139; ^{13}C NMR ($CDCl_3$) δ 12.5 and 12.7, 22.2. and 22.4, 39.2, 45.0, 49.5 and 49.7, 82.3, 103.8 and 104.0, 106.1 and 106.3, 115.1 and 115.4, 126.0, 127.9, 128.4, 137.1, 147.4 (d, J = 207), 158.2 (d, J = 242 Hz), 167.2, 175.3; IR (CH_2CH_2) 3430, 3300 (br), 3060, 2990, 2965, 2680, 1702, 1675, 1625, 1510, 1453, 1431, 1322, 1207, 1155, 1100, 1002, 800 cm^{-1}; HRMS calcd for $C_{20}H_{21}F_2N_2O_3$ ($M^+ + 1$): 375.1520. Found: 375.1539.

Synthesis of *N*-[(2*S*,1*R*)-2-(2,5-dichlorophenoxy)-1-methyl-2-phenylethyl]((4*S*,3*R*)-4-methyl-2-oxopyrrolidin-3-yl)carboxamide (23a)and *N*-[(2*S*,1*R*)-2-(2,5-dichlorophenoxy)-1-methyl-2-phenylethyl]((4*R*,3*S*)-4-methyl-2-oxopyrrolidin-3-yl)carboxamide (24a). A solution of 200 mg (1.4 mmol) methyl pyrrolidinone carboxylate **21**,[29] 0.6 mL (1.4 mmol) triethylamine, 470 mg (1.4 mmol) **8a**, and 220 mg (1.4 mmol) EDC in 10 mL CH_2CH_2 was stirred at room temperature overnight. Solvent was removed, and the residue was dissolved in EtOAc. The solution was washed with water and brine, dried ($MgSO_4$) and concentrated. The residue was chromatographed on silica gel (1:1 EtOAc–CH_2CH_2) to separate two materials. The higher R_f component (**23a**) was isolated as an oil: $[\alpha]_D^{25} = +9.0$ (c 1.03, EtOH); ^{1}H NMR ($CDCl_3$) δ 1.2 (d, 3H), 1.3 (d, 3H), 2.7–2.9 (m, 3H), 3.4–3.5 (m, 1H), 4.4 (m, 1H), 5.4 (m, 1H), 5.6 (s, 1H), 6.6 (s, 1H), 6.8 (d, 1H), 7.2–7.4 (m, 6H), 7.85 (d, 1H). ^{1}H NMR ($CDCl_3$) δ 1.2–1.3 (2d, 3H), 2.3–2.7 (m, 2H), 3.2 (m, 1H), 3.4 (m, 2H), 4.4 (m, 1H), 5.3 (dd, 1H), 5.7 (d, br 1H), 6.5 (m, 2H), 7.0 (m, 1H), 7.2–7.4 (m, 5H), 7.8 (2d, 1H); ^{13}C NMR ($CDCl_3$) δ 13.8, 20.5, 33.6, 48.4, 51.5, 53.6, 83.5, 116.2, 122.4, 122.7, 127.1, 129.0, 129.6, 131.5, 133.7 137.9, 154.9, 168.3, 176.0; IR (KBr) 3424 (br), 3276 (br), 1700, 1664, 1582, 1537, 1477, 1452, 1402, 1382, 1261, 1094, 1058, 996, 703 cm^{-1}; HRMS calcd for $C_{21}H_{23}Cl_2N_2O_3$ ($M^+ + 1$): 421.1086. Found: 421.1084. The lower R_f component (**24a**) was isolated as an oil: $[\alpha]_D^{25} = -23.4$ (c 1.02, EtOH); ^{1}H NMR ($CDCl_3$) δ 1.2 (d, 3H), 1.3 (d, 3H), 2.65 (d, 1H), 2.9 (m, 2H), 3.4–3.6 (m, 1H), 4.4 (m, 1H), 5.4 (s, 1H), 5.6 (s, 1H), 6.6 (s, 1H), 6.8 (d, 1H), 7.2–7.4 (m, 6H), 7.75 (d, 1H); ^{13}C NMR ($CDCl_3$) δ 13.1, 19.3, 32.4, 47.3, 50.4, 52.5, 82.5, 115.2, 121.3, 121.8, 125.9, 127.9, 128.5, 130.4, 132.6 136.8, 153.9, 167.1, 174.9; IR (KBr) 3424 (br), 3284 (br), 1700, 1658, 1582, 1539, 1477, 1452, 1402, 1261, 1094, 1060,

996, 702 cm^{-1}; HRMS calcd for $C_{21}H_{23}Cl_2N_2O_3$ ($M^+ + 1$): 421.1086. Found: 421.1090.

Synthesis of *N*-[(2*S*,1*R*)-2-(2,5-difluorophenoxy)-1-methyl-2-phenylethyl](4*S*,3*R*)-4-methyl-2-oxopyrrolidin-3-yl)carboxamide (23b) and *N*-[(2*S*,1*R*)-2-(2,5-difluorophenoxy)-1-methyl-2-phenylethyl](4*R*,3*S*)-4-methyl-2-oxopyrrolidin-3-yl)carboxamide (24b). A solution of 200 mg (1.4 mmol) methyl pyrrolidinone carboxylate **21**, 0.6 mL (1.4 mmol) triethylamine, 420 mg (1.4 mmol) **8b**, and 220 mg (1.4 mmol) EDC in 10 mL CH_2CH_2 was stirred at room temperature overnight. Solvent was removed, and the residue was dissolved in EtOAc. The solution was washed with water and brine, dried ($MgSO_4$) and concentrated. The residue was chromatographed on silica gel (1:1 EtOAc–CH_2CH_2) to separate two materials. The higher R_f component (**23b**) was isolated as a solid: mp 58–61 °C; $[\alpha]_D^{25} = +55.5$ (*c* 1.07, EtOH); ^{1}H NMR ($CDCl_3$) δ 1.2 (d, 3H), 1.3 (d, 3H), 2.7–3.0 (m, 3H), 3.4 (t, 1H), 4.4 (m, 1H), 5.3 (d, 1H), 5.65 (s, br, 1H), 6.4–6.6 (m, 2H), 6.9–7.0 (m, 1H), 7.2–7.4 (m, 5H), 7.85 (d, 1H); ^{19}F NMR ($CDCl_3$) δ−117,−140; ^{13}C NMR ($CDCl_3$) δ 13.7, 19.6, 32.6, 47.4, 50.5, 52.7, 83.3, 104.8, 107.3, 116.2, 126.3, 128.1, 128.6, 137.4, 137.4, 146.8, 149.1 (d, $J = 241$ Hz), 158.3 (d, $J = 245$ Hz), 167.3, 175.1; IR (CH_2CH_2) 3431, 3304 (br), 2985, 1702, 1668, 1532, 1511, 1453, 1432, 1321, 1207, 1155, 1100, 1002, 839, 802 cm^{-1}; HRMS calcd for $C_{21}H_{22}F_2N_2O_3$ ($M^+ + 1$): 389.1676. Found: 389.1671. The lower R_f component (**24b**) was isolated as a solid: mp 56–58 °C; $[\alpha]_D^{25} = -3.1$ (*c* 1.02, EtOH); ^{1}H NMR ($CDCl_3$) δ 1.2 (d, 3H), 1.3 (d, 3H), 2.7 (m, 1H), 2.9 (m, 2H), 3.45 (m, 1H), 4.4 (m, 1H), 5.4 (s, 1H), 5.6 (s, 1H), 6.4–6.6 (m, 2H), 7.0 (m, 1H), 7.2–7.4 (m, 5H), 7.75 (d, 1H); ^{19}F NMR ($CDCl_3$) δ −117, −140; ^{13}C NMR ($CDCl_3$) δ 13.4, 19.6, 32.4, 47.4, 50.7, 83.2, 104.7, 107.3, 116.3, 126.2, 128.1, 128.7, 137.3, 143, 149 (d, $J = 240$ Hz), 158 (d, $J = 240$ Hz), 167.2, 175.1; IR (CH_2CH_2) 3431, 3306 (br), 3059, 2985, 2961, 2677, 1702, 1675, 1627, 1511, 1453, 1431, 1322, 1207, 1155, 1100, 1002, 839, 801 cm^{-1}; HRMS calcd for $C_{21}H_{22}F_2N_2O_3$ ($M^+ + 1$): 389.1676. Found: 389.1676.

Synthesis of *N*-[(2*S*,1*R*)-2-(2,5-dichlorophenoxy)-1-methyl-2-phenylethyl](2-oxo(3-piperidyl))carboxamide (26a). A solution of 140 mg (1.0 mmol) valerolactam carboxylate **25**,[30] 0.28 mL (2.0 mmol) triethylamine, 330 mg (1.0 mmol) **8a**, and 190 mg (1.0 mmol) EDC in 10 mL CH_2CH_2 was stirred at room temperature overnight. The solution was washed with water and brine, dried ($MgSO_4$) and concentrated. The residue was chromatographed on silica gel (EtOAc) to give product as a 1:1 mixture of diastereomers as a solid: mp 54–64 °C; $[\alpha]_D^{25} = -6.8$ (*c* 1.17, EtOH); ^{1}H NMR ($CDCl_3$) δ 1.25 (m, 3H), 1.6–2.0 (m, 3H), 2.3 (m, 1H), 3.2 (m, 2H), 3.4 (m, 1H), 4.4 (m, 1H), 5.4 (dd, 1H), 6.0 (d, br 1H), 6.6 (d, 1H), 6.8 (m, 1H), 7.2–7.4 (m, 6H), 7.9 (2d, 1H); ^{13}C NMR ($CDCl_3$) δ 15.0 and 14.5; 22.0 and 21.7, 43.8 and 43.7, 47.7 and 47.6, 52.3 and 52.1, 83.9 and 83.8, 116.6, 122.8 and 122.7, 123.2, 127.5 and 127.3, 127.5, 129.9 and 129.3, 138.4, 155.5 and 155.4, 168.8 and 168.6, 171.8; IR (CH_2CH_2) 3400 (br), 3052, 2984, 2929, 2852, 1675, 1582, 1526, 1489, 1477, 1451, 1402, 1356, 1324, 1286, 1200, 1134, 1094, 1060, 997, 899,842, 805 cm^{-1}; HRMS calcd for $C_{21}H_{23}Cl_2N_2O_3$ ($M^+ + 1$): 421.1086. Found: 421.1087.

Synthesis of *N*-[(2*S*,1*R*)-2-(2,5-difluorophenoxy)-1-methyl-2-phenylethyl](2-oxo(3-piperidyl))carboxamide (26b). A solution of 140 mg (1.0 mmol) valerolactam carboxylate **25**, 0.28 mL (2.0 mmol) triethylamine, 300 mg (1.0 mmol) **8b**, and 190 mg (1.0 mmol) EDC in 10 mL CH_2CH_2 was stirred at room temperature overnight. The solution was washed with water and brine, dried ($MgSO_4$) and concentrated. The residue was chromatographed on silica gel (EtOAc) to give product as a 1:1 mixture of diastereomers as a solid: mp 52–58 °C; $[\alpha]_D^{25} = +29.4$ (*c* 1.02, EtOH); ^{1}H NMR ($CDCl_3$) δ 1.25 (m, 3H), 1.6–2.0 (m, 3H), 2.3–2.4 (m, 1H), 3.1–3.4 (m, 3H), 4.4 (m, 1H), 5.3 (dd, 1H), 5.9 (m, 1H), 6.5 (m, 2H), 7.0 (m, 1H), 7.2–7.4 (m, 5H), 7.9 (2d, 1H); ^{19}F NMR ($CDCl_3$) δ −117, −139; ^{13}C NMR ($CDCl_3$) δ 13.4 and 14.0, 20.4 and 20.7, 22.6, 42.5, 46.4, 50.5, 83.1 and 83.5, 104.7 and 105.1, 107.3, 126.3, 128.0, 128.6, 137.4, 146, 149 (d, $J = 240$ Hz), 158.3 (d, $J = 242$ Hz), 167.3 and 167.5, 170.7; IR (CH_2CH_2) 3400, 3300 (br), 3060, 2983, 2943, 2876, 1675, 1626, 1511, 1452, 1431, 1384, 1356, 1323, 1286, 1207, 1154, 1100, 1003, 839, 801 cm^{-1}; HRMS calcd for $C_{21}H_{22}F_2N_2O_3$ ($M^+ + 1$): 389.1676. Found: 389.1678.

Synthesis of 2-cyano-*N*-[(1R,2S)-2-(2,5-difluorophenoxy)-1-methyl-2-phenylethyl]-butanamide (5b). A few drops of DMF were added to a 10 mL CH_2Cl_2 solution of 115 mg (1.0 mmol) of 2-cyanobutanoic acid[20] and 0.086 mL (1.0 mmol) oxalyl chloride, and the mixture was stirred at room temperature overnight. A solution of 280 mg (0.84 mmol) **8b** and 0.26 mL (1.9 mmol) triethylamine in 10 mL CH_2Cl_2 was added. After stirring overnight, 1.0 g of Amberlite IRA-68 resin was added, and the mixture was filtered through a plug of silica gel rinsing through with EtOAc. The filtrate was stripped, and the residue was chromatographed (55% Et_2O–hexanes) to give 150 mg product as an oil that slowly solidified: mp 84–86 °C; $[\alpha]_D^{25} = +26.6$ (*c* 1.03, EtOH); ^{1}H NMR ($CDCl_3$) δ 1.0 and 1.1 (2d, $J = 7$ Hz, 3H), 1.25 (d, $J = 7$ Hz, 3H), 1.7–2.1 (m, 2H), 3.3–3.4 (m, 1H), 4.4 (m, 1H), 5.5 (m, 1H), 6.4 (m, 2H), 6.7–6.8 (m, 1H), 7.0 (m, 1H), 7.3–7.4 (m, 5H); ^{19}F NMR ($CDCl_3$) δ −117, −139; ^{13}C NMR ($CDCl_3$) δ 11.0 and 11.1, 13.6 and 13.9, 23.9, 40.1, 51.1 and 51.3, 83.3, 105.3 and 105.1, 108.1 and 108.0, 116.6 and 116.4, 117.9, 126.3, 128.6, 129.3 and 129.0, 136, 146.5, 147.6 (d, $J = 240$ Hz), 158.5 (d, $J = 244$), 154.2; IR (KBr) 3321, 2977, 2937, 2248, 1659, 1627, 1551, 1512, 1455, 1532, 1320, 1206, 1160, 1099, 794, 736, 707 cm^{-1}; HRMS calcd for $C_{20}H_{20}F_2N_2O_2$ ($M^+ + 1$): 359.1572. Found: 359.1571.

Acknowledgements

Recognition must be given to J. Michael Bonman and G. Shawn Smith for the in vivo rice blast disease control data described in this work.

References and Notes

1. Howard, R. H.; Valent, B. *Annu. Rev. Microbiol.* **1996**, *50*, 491.
2. Bechinger, C.; Giebel, K.-F.; Schnell, M.; Leiderer, P.; Deising, H. B.; Bastmeyer, M. *Science* **1999**, *285*, 1896.
3. Chumley, F. G.; Valent, B. *Mol. Plant-Microbe Interact.* **1990**, *3*, 135.
4. Basarab, G. S.; Steffens, J. J.; Wawrzak, Z.; Schwartz, R. S.; Lundqvist, T.; Jordan, D. B. *Biochemistry* **1999**, *38*, 6012.
5. Jordan, D. B.; Basarab, G. S. *Bioorg. Med. Chem. Lett.* **2000**, *10*, 23.
6. Jordan, D. B.; Zheng, Y.-J.; Locket, B. A.; Basarab, G. *S Biochemistry* **2000**, *39*, 2276.
7. Basarab, G. S.; Jordan, D. B.; Zheng, Y.-J. *Org. Lett.* **2000**, *2*, 1541.
8. Zheng, Y.-J.; Basarab, G. S.; Jordan, D. B. *Biochemistry* **2002**, *41*, 820.
9. Nakasako, M.; Motoyhama, T.; Kurahashi, Y.; Yamaguchi, I. *Biochemistry* **1998**, *37*, 9931.
10. Chen, J. M.; Xu, S. L.; Wawrzak, Z.; Basarab, G. S.; Jordan, D. B. *Biochemistry* **1998**, *37*, 17735.
11. Jordan, D. B.; Lessen, T.; Wawrzak, Z.; Bisaha, J. J.; Gehret, T. C.; Hansen, S. L.; Schwartz, R. S.; Basarab, G. S. *Bioorg. Med. Chem. Lett.* **1999**, *9*, 1607.
12. Basarab, G. S.; Jordan, D. B.; Gehret, T. C.; Schwartz, R. S.; Wawrzak, Z. *Biorg. Med. Chem. Lett.* **1999**, *9*, 1613.
13. Jennings, L. D.; Wawrzak, Z.; Amorose, D.; Schwartz, R.; Jordan, D. B. *Bioorg. Med. Chem. Lett.* **1999**, *9*, 2509.
14. Jennings, L. D.; Rayner, D. R.; Jordan, D. B.; Okonya, J. F.; Basarab, G. S.; Amorose, D. E.; Anaclerio, B. M.; Lee, J. K.; Schwartz, R. S.; Whitmore, K. A. *Bioorg. Med. Chem.* **2000**, *8*, 897.
15. Jordan, D. B.; Basarab, G. S.; Steffens, J. J.; Schwartz, R. S.; Doughty, J. G. *Biochemistry* **2000**, *39*, 8593.
16. Lundqvist, T.; Rice, J.; Hodge, C. N.; Basarab, G. S.; Pierce, J.; Lindqvist, Y. *Structure* **1994**, *2*, 937.
17. Wawrzak, Z.; Sandalova, T.; Steffens, J. J.; Basarab, G. S.; Lundqvist, T.; Lindqvist, Y.; Jordan, D. B. *Proteins: Struct., Funct. Gen.* **1999**, *35*, 425.
18. Gomez, J.; Freire, E. *J. Mol. Biol.* **1995**, *252*, 337.
19. Basarab, G. S. Unpublished results.
20. Winters, G.; Di Mola, N.; Oppici, E.; Nathansohn, G. *Farmaco Ed. Sci.* **1975**, *30*, 620.
21. Nishio, M.; Umezawa, Y.; Hirota, M.; Takeuchi, Y. *Tetrahedron* **1995**, *31*, 8665.
22. Bromilow, R. H.; Chamberlain, K. *Monogr.— Br. Plant Growth Regul. Group* **1989**, *18*, 113.
23. Lundqvist, T.; Weber, P. C.; Hodge, C. N.; Braswell, E. H.; Rice, J.; Pierce, J. *J. Mol. Biol.* **1993**, *232*, 999.
24. Schmidpeter, A.; Weinmaier, J. *Chem. Ber.* **1978**, *111*, 2086.
25. Chou, T. S.; Chang, R. C. *J. Chem. Soc., Chem. Commun.* **1992**, 549.
26. Mondon, A.; Oelrich, E.; Schickfluss, R. *Chem. Ber.* **1972**, *105*, 2036.
27. Wright, J. L.; Caprathe, B. W.; Downing, D. M.; Glase, S. A.; Heffner, T. G.; Jaen, J. C.; Johnson, S. J.; Kesten, S. R.; MacKenzie, R. G. *J. Med. Chem.* **1994**, *37*, 3523.
28. Hamashima, Y.; Ishikura, K.; Kubota, T.; Minami, K. *DE 3424780 A1, Chem. Abstr.* **1985**, *103*, 22372.
29. Hasegawa, M.; Nakayama, A.; Yokohama, S.; Hosokami, T.; Kurebayashi, Y.; Ikeda, T.; Shimoto, Y.; Ide, S.; Honda, Y.; Suzuki, N. *Chem. Pharm. Bull.* **1995**, *43*, 1125.
30. Narayanan, K.; Cook, J. M. *J. Org. Chem.* **1991**, *56*, 5733.